Discovery of a new chemical series of BRD4(1) inhibitors using protein-ligand docking and structure-guided design

Bryan C. Duffy, Shuang Liu, Gregory S. Martin, Ruifang Wang, Ming Min Hsia, He Zhao, Cheng Guo, Michael Ellis, John F. Quinn, Olesya A. Kharenko, Karen Norek, Emily M. Gesner, Peter R. Young, Kevin G. McLure, Gregory S. Wagner, Damodharan Lakshminarasimhan, Andre White, Robert K. Suto, Henrik C. Hansen, Douglas B. Kitchen

PII: S0960-894X(15)00452-7
DOI: http://dx.doi.org/10.1016/j.bmcl.2015.04.107
Reference: BMCL 22692

To appear in: *Bioorganic & Medicinal Chemistry Letters*

Received Date: 12 March 2015
Revised Date: 28 April 2015
Accepted Date: 30 April 2015

Please cite this article as: Duffy, B.C., Liu, S., Martin, G.S., Wang, R., Hsia, M.M., Zhao, H., Guo, C., Ellis, M., Quinn, J.F., Kharenko, O.A., Norek, K., Gesner, E.M., Young, P.R., McLure, K.G., Wagner, G.S., Lakshminarasimhan, D., White, A., Suto, R.K., Hansen, H.C., Kitchen, D.B., Discovery of a new chemical series of BRD4(1) inhibitors using protein-ligand docking and structure-guided design, *Bioorganic & Medicinal Chemistry Letters* (2015), doi: http://dx.doi.org/10.1016/j.bmcl.2015.04.107

Graphical Abstract

To create your abstract, type over the instructions in the template box below.
Fonts or abstract dimensions should not be changed or altered.

Discovery of a new chemical series of BRD4(1) inhibitors using protein-ligand docking and structure-guided design

Leave this area blank for abstract info.

Bryan C. Duffy, Shuang Liu, Gregory S. Martin, Ruifang Wang, Ming Min Hsia, He Zhao, Cheng Guo, Michael Ellis, John F. Quinn, Olesya A. Kharenko, Karen Norek, Emily M. Gesner, Peter R. Young, Kevin G. McLure, Gregory S. Wagner, Damodharan Lakshminarasimhan, Andre White, Robert K. Suto, Henrik C. Hansen, Douglas B. Kitchen*

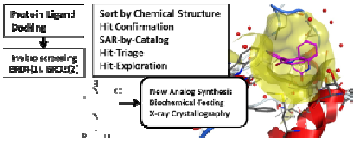

Bioorganic & Medicinal Chemistry Letters
journal homepage: www.elsevier.com

Discovery of a new chemical series of BRD4(1) inhibitors using protein-ligand docking and structure-guided design

Bryan C. Duffy[a], Shuang Liu[a], Gregory S. Martin[a], Ruifang Wang[a], Ming Min Hsia[a], He Zhao[a], Cheng Guo[a], Michael Ellis[a], John F. Quinn[b], Olesya A. Kharenko[c], Karen Norek[c], Emily M. Gesner[c], Peter R. Young[c], Kevin G. McLure[c], Gregory S. Wagner[c], Damodharan Lakshminarasimhan[d], Andre White[d], Robert K. Suto[d], Henrik C. Hansen[c], Douglas B. Kitchen[a*]

[a]*Albany Molecular Research (AMRI), 26 Corporate Circle, PO Box 15098, Albany, NY 12212-5098, USA*
[b]*JFQuinn Consulting, 113 Jay St. Albany, NY 12210*
[c]*Zenith Epigenetics Corp., Suite 300, 4820 Richard Road SW, Calgary, Alberta, T3E 6L1, Canada*
[d]*Xtal BioStructures, Inc., 12 Michigan Dr., Natick, MA 01760, USA*

* douglas.kitchen@amriglobal.com

ARTICLE INFO

Article history:
Received
Revised
Accepted
Available online
Keywords:
Virtual screening
Bromodomain inhibitors
BRD4(1)
Protein-ligand docking
Hit triage

ABSTRACT

Bromodomains are key transcriptional regulators that are thought to be druggable epigenetic targets for cancer, inflammation, diabetes and cardiovascular therapeutics. Of particular importance is the first of two bromodomains in bromodomain containing 4 protein (BRD4(1)). Protein-ligand docking in BRD4(1) was used to purchase a small, focused screening set of compounds possessing a large variety of core structures. Within this set, a small number of weak hits each contained a dihydroquinoxalinone ring system. We purchased other analogs with this ring system and further validated the new hit series and obtained improvement in binding inhibition. Limited exploration by new analog synthesis showed that the binding inhibition in a FRET assay could be improved to the low μM level making this new core a potential hit-to-lead series. Additionally, the predicted geometries of the initial hit and an improved analog were confirmed by X-ray co-crystallography with BRD4(1).

Bromodomains (BRDs) have recently been of increasing interest as possible new drug targets due to the profound effects these nuclear structures have on cellular transcriptional control. [1] BRD-containing proteins are key players in epigenetics by binding acetylated lysines (KAc) on chromatin structures and are thus termed "readers" of these epigenetic markers. Aberrant acetylation of lysine residues has been implicated in posttranslational increases of gene expression leading to several conditions, such as cancer, diabetes, inflammation and cardiovascular diseases. The BET (bromodomain and extra-terminal) protein family (BRD2, BRD3, BRD4 and BRDT) have two consecutive bromodomains that bind to proximal KAc sites on histone tails. BRDs contain well-defined pockets for KAc that provide a "druggable" site suitable for small molecule inhibitor development. Many examples of potent BRD binders have been disclosed and are illustrated as scaffolds **1-5** and specific optimized examples, **6-9** (adapted from Filippakopoulos and Knapp). 1

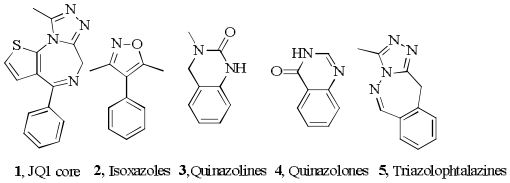

1, JQ1 core **2**, Isoxazoles **3**, Quinazolines **4**, Quinazolones **5**, Triazolophtalazines

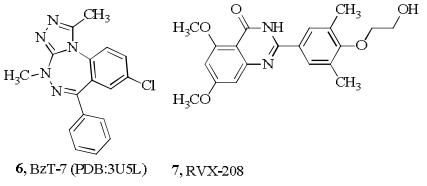

6, BzT-7 (PDB:3U5L) **7**, RVX-208

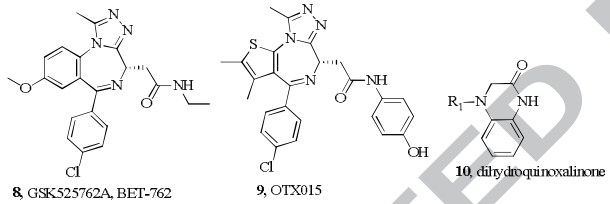

8, GSK525762A, BET-762 **9**, OTX015 **10**, dihydroquinoxalinone

In an effort to identify new starting points for a BRD inhibitor program, we undertook virtual screening using protein-ligand docking and tested selected compounds using two competitive binding inhibition assays and identified a new core ring system, **10**, as a possible starting point for drug discovery. Herein, we report the validation of the binding activities of this series, crystallographic confirmation of the binding mode in BRD4(1) and a limited SAR exploration around this new N-substituted dihydroquinoxalinone hit series.

Screening strategy: Our goal in this hit-to-lead program was to rapidly identify new starting compound scaffolds using small focused sets of readily available samples with diverse structural cores which inhibit the binding of histones to the BRD4(1) domain. Virtual screening is a common method for the generation of hit compounds in medicinal chemistry [2, 3] and recently has been used to identify compounds that bind to bromodomains. [4, 5, 6] To rapidly identify new hits, we chose to virtually screen a collection of chemical structures and then purchased and tested samples for binding activity in BRD4(1) and BRD2(2). We used the concept of the "latent-hit series" [7] to overcome the inherent errors in docking, scoring and single concentration screening.

Figure 1. Screening Process. 153 compounds were selected by docking and purchased. After testing in BRD2(2) and BRD4(1) single point assays scaffold **11** was identified and rapidly explored by additional compound purchases.

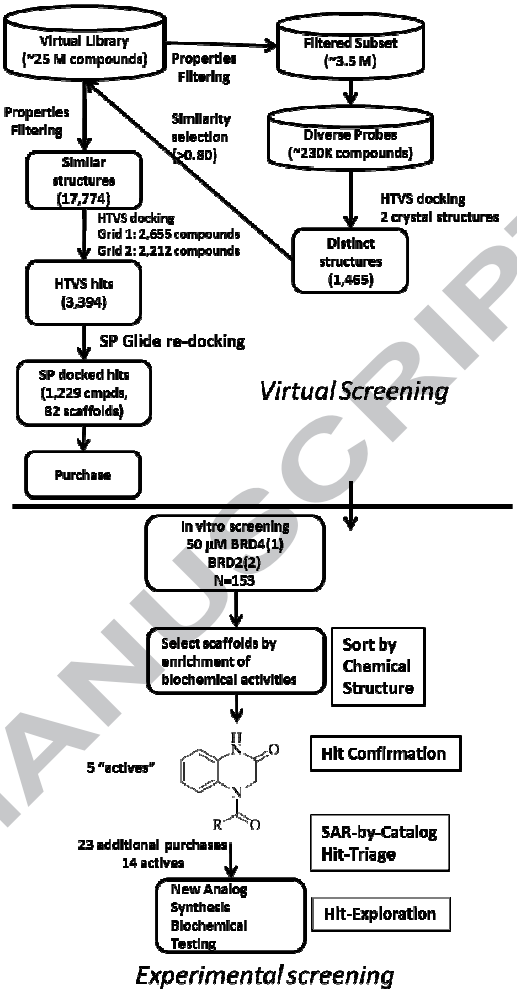

First, we designed our workflow to use 3D protein structural information in order to test only a few samples while simultaneously accounting for docking inaccuracies, unavailable compounds and experimental uncertainties. Docking scores from any available algorithm have large errors in predicting binding potency. However, we believed that if many examples from a scaffold score well in docking calculations that it is less likely that all the high scores are incorrect. Therefore, we attempted to identify clusters of chemically similar compounds containing common core scaffolds with significantly higher docking scores and simultaneously to improve the chances that examples of each scaffold were available for purchase and testing. Experimental uncertainties arise from multiple sources including weighing, structural assignment and biochemical measurements. In order to decrease the chances of missing an active compound as a false negative, clusters of screening compounds provide statistical reinforcement of single concentration screening data, and possibly provide a small amount of early SAR. Grouping experimental measurements by scaffold can identify active substructures where no single member achieved high inhibition in the single point binding assay. As hits were identified, chemical structures were grouped by common scaffolds. The structural similarity within each scaffold provided confidence that the weak activity measurements were valid and that the structural representations were likely accurate. Additionally, when similar binding activity exists within a series, fewer analogs need to be re-synthesized since any example becomes

validation of the series and synthetic efforts can be focused on new analogs. Compounds obtained in virtual screening have been previously disclosed and therefore, do not offer novel chemical structures. However, each scaffold can be used as rapid entry points to identify novel BRD4(1) hit series. Our subsequent goal of the hit-to-lead program was to rapidly develop structure activity relationships (SAR) on each biologically active scaffold yielding scaffolds with multiple members for further lead optimization.

Figure 2. Initial co-crystal structures of BRD4(1) used for docking. Top panel: co-crystal of **7** 8 ; Lower panel: pdb code: 3u5l, **6**. Water molecule, HOH4 (blue) was the only water molecule retained in the docking models.

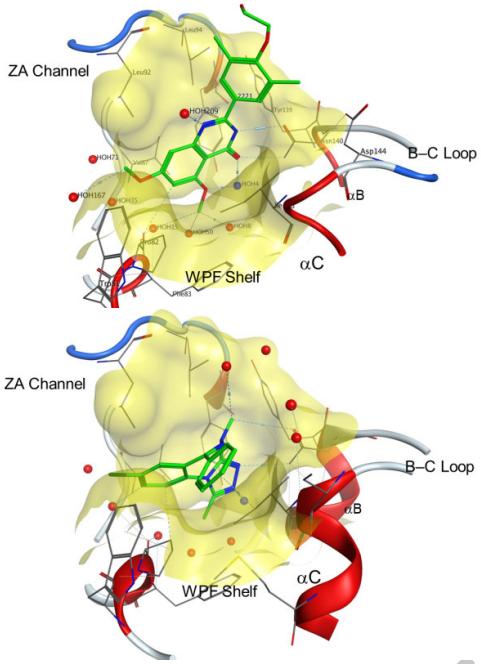

Virtual Screening Method: Ligands are known to induce differences in shape among crystal structures and this in turn changes the structure and binding energy predictions of any docking protocol. In order to increase the chances that we would identify new diverse scaffolds for BRD4(1), we used two X-ray crystal structure models with different co-crystallized ligand structural classes: an analog of RVX-208 (**7**) with binding site coordinates similar to RVX-208 and **6**, BzT-7 (PDB:3u5l) 9 which occupies an additional pocket. The docking grids were prepared using Schrödinger's protein preparation tools and Glide grid preparation workflows for each crystal structure. 10 In both docking models, only one water molecule (HOH4) was retained from each crystal structure (Figure 2). 9, 8, 11 This water molecule is in the chain of five commonly conserved water molecules and is the closest water to Asn140. It bridges Tyr97 and the ligand through hydrogen bonds in both X-ray crystal structures. Elimination of all other water molecules provided room for new interactions.

Virtual Screening to identify potential hit series: The virtual screening and hit triage process that we used is illustrated in Figure 1. A source library of ~25 million compounds from various publically available sources was filtered on common drug-like property criteria. A diverse-set of ~230,000 compounds was selected through multiple rounds of random selections followed by confirmation of diversity through 2-D atom-pair similarity calculations. 12 Compounds within each selection subset had 2D atom-pair similarity Dice coefficients of less than 0.60. The diverse set was not strictly filtered to prevent the elimination of compounds that do not have optimal R-groups, but could lead to groups of more ideal compounds by using chemical similarity calculations.

The protein-ligand docking proceeded as illustrated in Figure 1 starting from a diverse set of available compounds with successive rounds of higher precision docking.[27] Compounds within each of the top-scoring scaffolds were manually viewed and evaluated as to the likelihood of binding with valid poses and distinguishing features from known BRD binding compounds. The minimum requirement for consideration as a valid pose was a predicted potential hydrogen bond to the Asn140 sidechain amide, which mimics the native histone acetylated lysine binding location. Compounds with groups residing in the WPF shelf were given special attention. A total of 153 available compounds met the hydrogen bond requirements and either a very favorable Glide score or were members of a scaffold having a favorable average Glide score. These compounds represented 82 scaffolds and were purchased from commercial vendors and evaluated in in vitro screening.

Chart 1. Initial hits obtained in single concentration BRD4(1) and BRD2(2) per cent inhibition measurements.

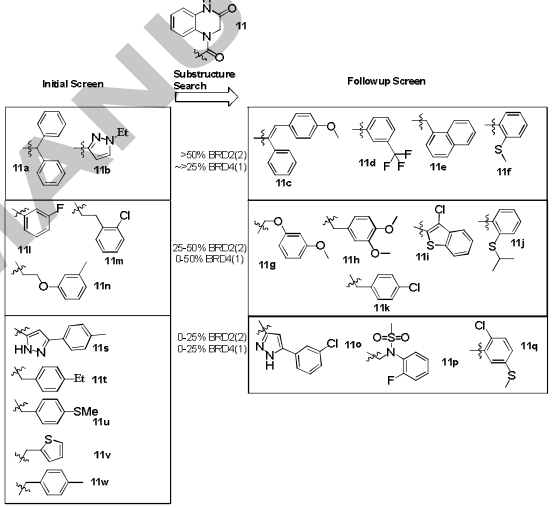

Hit Screening and treatment: The purchased compounds were initially tested by HTRF binding inhibition to BRD4(1) and BRD2(2) at 50 µM concentrations.[28] Compounds with greater than 50% binding to BRD4(1) were submitted for dose-response testing and IC_{50} calculations, while hits in the 30–49% binding range at 50 µM were grouped by scaffold.

We grouped compounds into top-level scaffolds (most complex) and the next lower sub-scaffolds (removal of one ring). 13 The enrichment of the occurrence of hits (binding >30%) within a scaffold was used to indicate likely hit series for further SAR exploration. These few compounds are only indicative of potential active scaffolds but the fact that there is significant enrichment of hits overcomes the otherwise high experimental uncertainty.

Compounds containing the N-acylated dihydroquinoxalone ring, **11**, showed promising activity and we will only discuss further SAR work on this scaffold, though several other series were also obtained from the virtual screening. Additional purchases were made within the series following the same docking protocol. Of the 22 tested dihydroquinoxalones, 14 exhibited inhibition in either BRD4(1) or BRD2(2) assays. Chart 1 divides the structures into three groups: strong inhibitors in at

least one assay (>50% inhibition), weak hits (25-50% inhibition in one assay) and very weak hits that lack meaningful inhibition. The % inhibition of binding to BRD2(2) was generally higher than to BRD4(1) with the dihydroquinoxalone system. BRD2(2) was inhibited in the 50-75% range for four compounds whereas the inhibition was ~0-25% in BRD4(1). Even though our ultimate goal was BRD4(1) inhibition, the addition of testing in BRD2(2) provided validation for hits near the activity cutoff which would have been missed using only one assay.

Structure-Activity exploration: The compound **11c** was the most active compound from the hit series after single concentration testing. To begin to explore the series, we first resynthesized **11c** and retested to obtain more accurate IC_{50}'s. In parallel with synthetic expansion of the series, a resynthesized sample of **11c(16a)** was co-crystallized in BRD4(1). [29] (Figure 3, PDB:4hy3) The X-ray crystal structure was important to the screening process, because it established that the weak hit was binding in the desired pocket in a manner that agreed with the Glide docking SP pose with an rmsd of 0.96 Å from the predicted geometry. The structure also provided the initial information to suggest improvements in the binding interactions of **16a** (22 µM, BRD2(2) see Table 1). The –NH group of the dihydroquinoxaline forms a hydrogen bond to the BRD4(1) Asn140 sidechain in a manner similar to the native acetylated lysine and other inhibitor structures (see figures ref 1 and pdb codes 3uvw and 3u5l.). The pendant aryl system points towards the WPF shelf while the carbonyl of the amide group points to the narrow ZA water channel. The SAR exploration for this scaffold attempted to enhance these three interaction points and to identify any freedom to eliminate liabilities in the series.

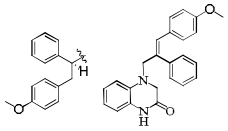

11x **10a**

The initial hit, **11c** contains some possible liabilities to development into a true lead series. The potential Michael acceptor, the enone moeity was the first concern. We made an analog where the double bond was hydrogenated to provide **11x**. Additionally, the necessity of the carbonyl was examined with **10a**. In both cases, the inhibition was < 30% at 50 µM suggesting that a planar geometry was necessary at both the amide and vinyl group. Additional, analogs that are not reported here support these trends.

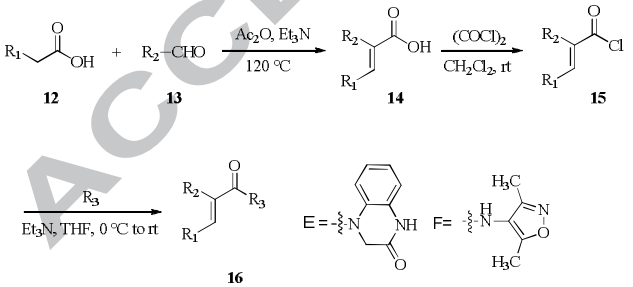

12 **13** **14** **15** **16**

Scheme 1. Synthesis of **16a-n**.[30]

Table 1. FRET binding data for α,β-unsaturated amides

Compd.	*Substitution*			*IC50 (µM)*[a]	
	R^1	R^2	R^3	BRD4(1)	BRD2(2)
11c, 16a	4-MeOPh	Ph	E	26	22
16b	4-MeO-Ph	thiophen-2-yl	E	13 (2)	23 (2)
16c	4-MeO-Ph	4-acetamido-Ph	E	13	24
16d	4-MeO-Ph	4-MeO-Ph	7-MeO-E	13	13
16e	4-MeO-Ph	3,4-di-Me-Ph	E	14 (2)	>50 (2)
16f	4-MeO-Ph	4-MeO-Ph	E	16 (2)	13 (2)
16g	4-MeO-Ph	3,4-di-MeO-Ph	E	18	26
16h	4-pyridyl	4-MeO-Ph	E	25	5
16i	4-MeO_2C-Ph	Ph	E	25 (2)	25 (2)
16j	4-MeO-Ph	Ph	7-MeO-E	34 (2)	>50 (2)
16k	3-NHCOMe	Ph	E	40	10
16l	4-MeO-Ph	4-MeO-Ph	F	44	12
16m	4-NH_2COPh	Ph	E	46	49
16n	4-MeOPh	2,4-di-OMe-Ph	E	>50	>50

[a] n=1 unless otherwise indicated in parenthesis

A small set of compounds similar to amide **11c**(**16a)** were synthesized in order to complement the purchased compounds and verify that the observed activity was derived from the chemical structure and was representative of a larger series of compounds. A three-step reaction sequence was used to prepare and test a small library of compounds for testing primarily intended to optimize binding through changes in R^1 and R^2 (Scheme 1).

Based on initial modeling of the series and the crystal structures, R^1 was expected to rest on the WPF shelf. R^2 was expected to face a narrow water channel (the ZA channel). R^3 was varied in order to explore the hydrogen bonding opportunities close to Asn140. The compounds were tested in the BRD4(1) and BRD2(2) HTRF binding assays (Table 1). The SAR was flat and narrow, however, significant improvement in binding was observed with the best examples achieving 13 µM binding inhibition for BRD4(1). Compounds with the electron rich 4-methoxyphenyl as R^1 and substituted phenyl groups as R^2 performed the best in the binding assay.

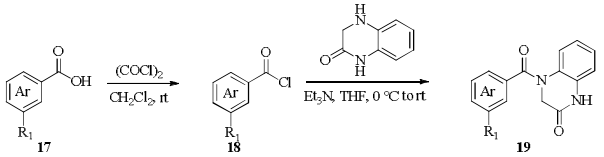

17 **18** **19**

Scheme 2. Synthesis of **19a–i**.

A small series of compounds related to scaffold **19** and analogs of compound **16a** were prepared and tested (Table 2). These aryl amides were prepared using the route in Scheme 2, in an effort to replace the α,β-unsaturation with alternate, less-reactive biaryl groups and to introduce a scaffold that had not been disclosed previously. The 5-Ar position for R^1 was predicted to point towards the WPF shelf with the expectation of improving binding. Docked pose predictions of the pyridyl-phenyl group of **19d** were ambiguous in multiple protein sites because of very similar scores. Some of the docked poses filled the ZA channel with the pyridyl-phenyl ring while other models accommodated the same ring system in the WPF shelf. Therefore, **19d** was prepared and submitted for co-crystallization with BRD4(1) and the X-ray crystal structure determined (pdb:4hy4). The X-ray crystal structure reveals that one of the

ring bonds of the pyridine ring replaces the double bond of the α,β-unsaturated amide (see Figure 3c) as predicted by some of the docked models of **19d**. This observation confirms the necessity of two sp2 centers. The X-ray crystal structure (Figure 3) indicates a stabilizing hydrogen bond between the 3-pyridyl nitrogen atom and a water molecule in the ZA channel that was not present in any of the crystal structures used for docking (Scheme 2). In fact, the chlorine atom of **6** in its crystal structure (3u5l) is located in approximately the same location as this new water molecule. Additionally, the water molecule initiates a hydrogen-bond chain with other water molecules that form hydrogen bonds to the protein. The most potent compound of this series, **19a**, replaced this 3-pyridyl group with a 3-hydroxy group that is predicted to form a hydrogen bond to the same water network and a modest improvement in binding was observed.

Table 2. FRET binding data for biaryl amides.

Compd.	*Substitution*		*IC50 (μM)*[a]	
	R[1]	Ar	BRD4(1)	BRD2(2)
19a	Ph	3-hydroxyPh	9	nd
19b	Ph	3-MeO-Ph	13	nd
19c	3-MeO-Ph	3-pyridyl	25	nd
19d	Ph	3-pyridyl	26	20.
19e	3-hydroxyPh	3-pyridyl	29	nd
19f	3-cyanoPh	3-pyridyl	44	12
19g	4-F-Ph	3-pyridyl	47	nd
19h	4-Cl-Ph	3-pyridyl	49	nd
19i	PhCH2NH-	3-MeO-Ph	>50	nd

[a] nd= no data; n=1 in all cases

A new hit series was identified for inhibition of BRD4(1), an important new biological target. We used docking to identify a series of hits that were confirmed by a limited SAR exploration and two protein co-crystal structures. The hit identification step used compound clustering extensively to improve the quality of virtual screening and the probability of a successful selection of active compounds for purchase. Scaffold relationships and latent-hit analysis increased the probability of selecting true-positive clusters of active compounds, while decreasing the probability of selecting false-positive clusters. The confirmation of ligand binding pose through X-ray crystallography validated the docking model predictions and identified regions where improved binding may be possible. We improved the best initial screening activity from 26 μM (**11c**) to 9 μM (**19a**) in BRD4(1) inhibition. The application of virtual screening, cheminformatic techniques, X-ray crystallography, and early focused library synthesis rapidly identified several scaffold clusters of BRD4(1) binding hits derived from commercially available compounds that may act as starting points for medicinal chemistry hit-to-lead optimization. Other clusters of compounds are being pursued in parallel.

Figure 3. X-ray crystal structures of **11c** (**16a)** (top) and **19d** (middle) and both molecules (bottom) in BRD4(1). Water molecules are colored green in the bottom image for 11c structure. (PDB:4hy3 and 4hy4)

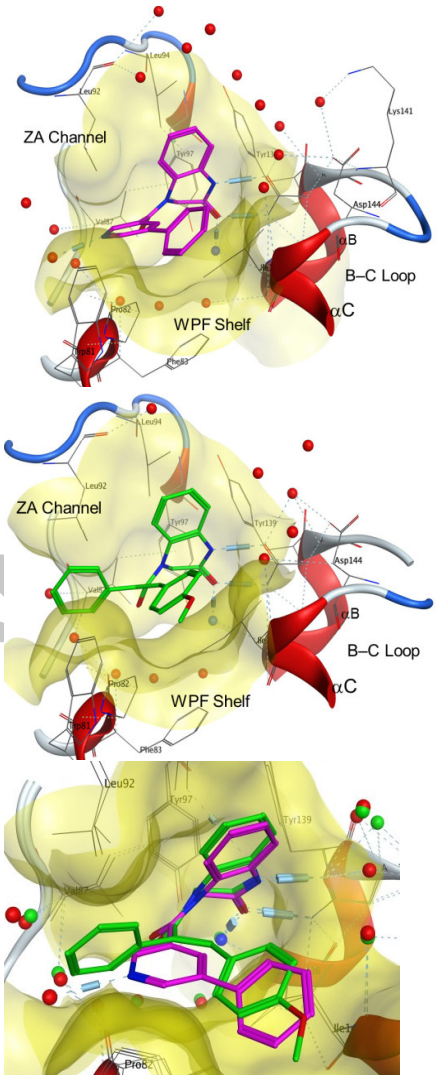

Acknowledgements

We thank Hélène Decornez and Keith Barnes for careful reading of the manuscript.

References and Notes

1. Filippakopoulos, P.; Knapp, S. *Nat. Rev. Drug Disc.* **2014,** *13* 337.
2. Kitchen, D. B.; Decornez, H.; Furr, J. R.; Bajorath, J. *Nat.Rev.Drug Disc.* **2004,** *3* 935.
3. Lavecchia, A.; Di Giovanni, C. *Curr.Med.Chem.* **2013,** *20* 2839.
4. Vidler, L. R.; Filippakopoulos, P.; Fedorov, O.; Picaud, S.; Martin, S.; Tomsett, M.; Woodward, H.; Brown, N.; Knapp, S.; Hoelder, S. *J. Med. Chem.* **2013,** *56* 8073.
5. Muwa, C.; Singam, E. R. A.; Raman, S. S.; Subramanian, V. *Mol. BioSy.s* **2014,** *10* 2384.
6. Pachaiyappan, B.; Woster, P. M. *Bioorg. Med. Chem. Lett.* **2014,** *24* 21.
7. Varin, T.; Didiot, M. C.; Parker, C. N.; Schuffenhauer, A. *J. Med. Chem.* **2012,** *55* 1161.
8. Filippakopoiulos, P.; Picaud, S.; Federov, O.; Keller, M.; Wrobel, M.; Morgenstern, O.; Bracher, F.; Knapp, S. *Bioorg. Med. Chem.* **2012,** *20* 1878.
9. *Suite 2012: Glide, version 5.8;* Schrodinger, LLC: New York, NY, 2012.
10. McLure, K. G.; Gesner, E. M.; Tsujikawa, L.; Kharenko, O. A.; Attwell, S.; Campeau, E.; Wasiak, S.; Stein, A.; White, A.; Fontano, E.; Suto, R. K.; Wong, N. C. W.; Wagner, G. S.; Hansen, H. C.; Young, P. R. *PLOS One* **2013,** *8* e83190.
11. Vidler, L. R.; Brown, N.; Knapp, S.; Hoelder, S. *J. Med. Chem.* **2012,** *55* 7346.
12. Carhart, R. E.; Smith, D. H.; Venkataraghavan, R. *J. Chem. Inf. Comput. Sci.* **1985,** *25* 64.
13. Wilkens, S. J.; Janes, J.; Su, A. I. *J. Med. Chem.* **2005,** *48* 3182.
14. Zhao, H.; Gartenmann, L.; Dong, J.; Spiliotopoulos, D.; Caflisch, A. *Bioorg. Med. Chem. Lett*. **2014,** *24* 2493.
15. Pachaiyappan, B.; Woster, P. M. *Bioorg. Med. Chem. Lett.* **2014,** *24* 21.
16. Herold, J. M.; Wigle, T. J.; Norris, J. L.; Lam, R.; Korboukh, V. K.; Gao, C.; Ingerman, L. A.; Kireev, D. B.; Senisterra, G.; Vadadi, M.; Tripathy, A.; Brown, P. J.; Arrowsmith, C. H.; Jin, J.; Janzen, W. P.; Frye, S. V. *J. Med. Chem.* **2011,** *54* 2504.
17. Filippakopoulos, P.; Knapp, S. *Nat. Rev. Drug Disc.* **2014,** *13* 337.
18. Chung, C.-w.; Dean, A. W.; Woolven, J. M.; Bamborough, P. *J. Med. Chem.* **2012,** *55* 576.
19. Duffy, B. C.; Zhu, L.; Decornez, H.; Kitchen, D. B. *Bioorg. Med. Chem.* **2012,** *20* 5324.
20. Mujtaba, S.; Zeng, L.; Zhou, M.-M. *Oncogene* **2007,** *26* 5521.
21. Friesner, R. A.; Murphy, R. B.; Repasky, M. P.; Frye, L. L.; Greenwood, J. R.; Halgren, T. A.; Sanschagrin, P. C.; Mainz, D. T. *J. Med. Chem.* **2006,** *49* 6177.
22. Halgren, T. A.; Murphy, R. B.; Friesner, R. A.; Beard, H. S.; Frye, L. L.; Pollard, W. T.; Banks, J. L. *J. Med. Chem.* **2004,** *47* 1750.
23. Friesner, R. A.; Banks, J. L.; Murphy, R. B.; Halgren, T. A.; Klicic, J. J.; Mainz, D. T.; Repasky, M. P.; Knoll, E. H.; Shaw, D. E.; Shelley, M.; Perry, J. K.; Francis, P.; Shenkin, P. S. *J. Med. Chem.* **2004,** *47* 1739.
24. Otwinowski, Z.; Minor, W. *Methods Enzymol.* **1997,** *276* 307.
25. Vagin, A. A.; Steiner, R. S.; Lebedev, A. A.; Potterton, L.; McNicholas, S.; Long, F.; Murshudov, G. N. *Acta Crystallogr., Sect. D* **2004,** *60* 2284.
26. Emsley, P.; Cowtan, K. *Acta Crystallogr., Sect. D* **1991,** *60* 2126.

[27] The diverse set of 230,000 compounds was docked into each independent BRD4(1) docking models using Schrödinger's Glide program in the high throughput virtual screen (HTVS) mode. 25' 24 Poses of compounds with a Glide score less than -7.5 in either model were retained. This diverse set of 1,475 compounds was used to select compounds from the virtual library with 2D atom pair similarity scores ≥0.80 Dice similarity level. These similarity calculations resulted in 17,774 compounds and the compounds were filtered using the same property values and this filtering resulted in a total of 3394 molecules. The HTVS selection set of compounds was re-docked at the Glide Standard Precision(SP) precision level for more accurate scoring. The top scoring 1,229 compounds from both grids contained 82 top-level HierS scaffolds. 13

[28] **Bromodomain expression**: BRD4(1) and BRD2(2) bromodomain constructs were based on (Filippakopoulos et al., 2010, Nicodeme et al., 2010) with an added N-terminal His-tag. These constructs were cloned, expressed, and purified by nickel affinity and size exclusion chromatography by either Genscript or Xtal BioStructures, frozen at -80 °C for competition experiments. **Time Resolved Fluorescence Resonance Energy Transfer (TR-FRET) assay**: 200 nM N-terminally His-tagged bromodomains, BRD4(1) or BRD2(2) and 25-50 nM biotinylated tetra-acetylated histone H4 peptide (Millipore) were incubated in the presence of Europium Cryptate-labeled streptavidin (Cisbio Cat. #610SAKLB) and XL665-labeled monoclonal anti-His antibody (Cisbio Cat.#61HISXLB) in a white 96 well microtiter plate (Greiner). For inhibition assays, serially diluted compound was added to these reactions in a 0.2% final concentration of DMSO. Final buffer concentrations were 30 mM HEPES pH 7.4, 30 mM NaCl, 0.3 mM CHAPS, 20 mM PO4 pH 7.0, 320 mM KF, 0.08% BSA). After 2h incubation at room temperature, the fluorescence by FRET was measured at 665 and 620 nm by a SynergyH4 plate reader (Biotek). Duplicate measurements were obtained at each concentration. IC_{50} values were determined from a dose response curve.

[29] **X-ray Crystallography**. The recombinant human BRD4(1) 8 protein at 1 mg/mL was mixed with 0.6 mM **16a** from 100 mM DMSO stock. The complex was incubated at room temperature for 30 min and then concentrated to 4.0 mg/mL using 3000MWCO concentrators. Protein co-crystals were obtained by vapor diffusion with sitting drops against a reservoir solution containing 200 mM Potassium thiocyanate and 20% (W/V) PEG 3350. Selected monocrystals were briefly treated with a cryo-protectant solution containing the well solution supplemented with 20% 2-methyl-2,4-pentanediol and flash-frozen in liquid nitrogen.

Apo-BRD4(1) crystals were obtained by vapor diffusion using sitting drop against a reservoir solution containing 10% (W/V) PEG 3350, 100 mM HEPES pH 7.5 and 200 mM L-proline. Well-formed crystals were soaked for 3 hours at room temperature with the same reservoir solution supplemented with 20 mM **19d**. Soaked crystals were briefly treated with the soaked solution where the PEG3350 concentration was increased to 35% (W/V) and flash-frozen in liquid nitrogen.

Single-crystal X-ray diffraction was obtained at Beam line X29 of the National Synchrotron Light Source, Brookhaven National Laboratory, using an automated sample mount system. The X-ray diffraction data were reduced using HKL2000 26 The BRD4(1)-**16a** and BRD4(1)-**19d** crystals both belonged to the space group P212121 and they diffracted to 1.33 Å and 1.60 Å resolution, respectively (Table S1). The protein structures were solved by molecular replacement and refined using REFMAC5 22 as previously done. 8 Model rebuilding was pursued using COOT 23. In each structure, a single compound conformation was observed and refined. The BRD4(1)-**19d** co-structure was refined to an R/Rfree of 16.0%/19.9% with good stereochemistry. Given the high resolution of the BRD4(1)-**16a** co-structure, individual anisotropic temperature factors were also refined to an R/Rfree of 11.0%/14.8% with good stereochemistry. The final crystallographic data reduction statistics are summarized in Table S2. The structures have been deposited in the PDB with the following codes: 4yh3 and 4yh4.

[30] The synthesis of these analogues is exemplified by the preparation of **16e** as described below:

Step 1: A mixture of 4-methoxybenzaldehyde (1.36 g, 10.0 mmol), 2-(4-methoxyphenyl)acetic acid (1.66 g, 10.0 mmol), acetic anhydride (2.04 g, 20.0 mmol), and triethylamine (1.0 mL, 7.0 mmol) was heated at 140 °C under nitrogen for 16 h. The reaction

mixture was cooled to room temperature and diluted with ethyl acetate and water. The organic layer was washed with brine, dried over sodium sulfate, filtered and concentrated. The residue was recrystallized in ethyl acetate and hexanes to afford (*E*)-2,3-bis(4-methoxyphenyl)acrylic acid (0.65 g, 23%) as a yellow solid: ^{1}H NMR (500 MHz, $CDCl_3$) δ 7.87 (s, 1H), 7.17 (dd, *J* = 6.7, 2.1 Hz, 2H), 7.05 (dd, *J* = 7.0, 1.9 Hz, 2H), 6.93 (dd, *J* = 6.7, 2.1 Hz, 2H), 6.71 (dd, *J* = 7.0, 2.0 Hz, 2H), 3.85 (s, 3H), 3.77 (s, 3H).

Step 2&3: To a solution of (*E*)-2,3-bis(4-methoxyphenyl)acrylic acid (142 mg, 0.5 mmol) in dichloromethane (3 mL) was added oxalyl chloride (0.17 mL, 2.0 mmol). The reaction mixture was stirred at room temperature for 1 h and then concentrated. The residue was dissolved in tetrahydrofuran (2 mL) and was added into an ice cold solution of 3,4-dihydroquinoxalin-2(1*H*)-one (67 mg, 0.45 mmol) and triethylamine (50 mg, 0.5 mmol) in tetrahydrofuran (7 mL). The mixture was warm to room temperature, stirred for 16 h. The mixture was diluted with ethyl acetate and saturated sodium carbonate (200 mL/50 mL). The organic layer was separated, washed with brine, dried over sodium sulfate, filtered and concentrated. The residue was purified by chromatography (silica gel, 0–40% ethyl acetate/hexanes) to give **Example 16e** (170 mg, 82%) as an off-white solid: ^{1}H NMR (500 MHz, DMSO–d_6) δ 10.57 (s, 1H), 7.43 (d, *J* = 8.0 Hz, 1H), 7.06 (td, *J* = 7.7, 1.3 Hz, 1H), 7.01–6.99 (m, 4H), 6.94 (td, *J* = 7.9, 1.3 Hz, 1H), 6.86 (dd, *J* = 7.9, 1.2 Hz, 1H), 6.81–6.76 (m, 5H), 4.34 (s, 2H), 3.71 (s, 3H), 3.70 (s, 3H); ESI *m/z* 415 $[M + H]^+$.